

# Evidence for $\text{Mn}^{2+}$ fine structure in $\text{CdMnSe}/\text{ZnSe}$ quantum dots caused by their low dimensionality

P. G. Baranov<sup>1)</sup>, N. G. Romanov, D. O. Tolmachev, R. A. Babunts, B. R. Namozov, Yu. G. Kusrayev, I. V. Sedova, S. V. Sorokin, S. V. Ivanov

*Ioffe Physical-Technical Institute, 194021 St. Petersburg, Russia*

Submitted 1 September 2008

Resubmitted 24 September 2008

The axial fine structure with strong positive zero-field splitting for  $\text{Mn}^{2+}$  ions in  $\text{CdMnSe}/\text{ZnSe}$  quantum dots caused by their low dimensionality was revealed. Magnetic resonance was measured as a variation of photoluminescence intensity. In spite of isotropic  $g$  factor of  $\text{Mn}^{2+}$  ions, the anisotropic behavior of the center of gravity of the resonance has been observed because of the high Boltzmann factor at 35 GHz and 2 K.

PACS: 75.50.Pp, 75.75.+a, 78.67.Hc

The most extensively studied semimagnetic semiconductors are II-VI compounds in which a fraction of the group II sublattice is replaced at random by Mn [1]. The exciting recent developments in the field of semimagnetic II-VI semiconductors, presenting an entirely new physics, is the preparation of low-dimensional structures: quantum wells, superlattices (SL's) and quantum dots (QD's).

The zinc blende and wurtzite crystal structures are both formed with tetragonal  $sp^3$  bonding, involving the two valence  $s$  electrons of the group II element and the six valence  $p$  electrons of the group VI elements. The ease with which Mn atoms substitute for the group II elements in these structures results from the fact that the free Mn atom has the  $3d^5 4s^2$  configuration with valence electrons corresponding to  $4s^2$  orbital and the  $3d$  orbitals of Mn are exactly half-filled. By Hund's rule all five  $3d$  spins are parallel, and it would require considerable energy to add an electron with opposite spin to the Mn atom. In this sense the  $3d^5$  orbit acts as a complete shell (like  $3d^{10}$  or  $4d^{10}$  shells in Zn or Cd), and the Mn atom is thus more likely to resemble a group II element in its behavior. Mn contributes its  $4s^2$  electrons to the  $sp^3$  bonding, and can therefore substitutionally replace the group II elements in tetrahedral structures. The ground state  $^6S$  ( $S=5/2$ ,  $L=0$ ) is spherically symmetrical and orbitally nondegenerate, and in the crystal field notation is labelled as  $^6A_1$ . The lowest-energy excited level for a free Mn atom is the nine-fold degenerate  $^4G$  state ( $S=3/2$ ,  $L=4$ ) which is split into four levels with the lowest  $^4T_1$  state. Transitions between the ground state and any of excited states in

the free Mn atom are forbidden by the  $S=0$  and parity selection rules. However, for  $\text{Mn}^{2+}$  ions in the II-VI matrix the selection rules are relaxed and, as a result, the transition from the  $^6A_1$  level to the lowest excited  $^4T_1$  state becomes possible (it corresponds to  $\sim 2.2$  eV).

Incorporation of Mn atoms into II-VI semiconductors modifies their optical and magnetic properties due to the exchange interaction of the localized  $\text{Mn}^{2+}$  magnetic moment of the  $3d^5$  electrons with band  $sp$  electrons. The  $sp-d$  exchange interaction influences physical phenomena which involve electrons in the conduction and valence bands, e.g., the giant Zeeman splitting of both the conducting and valence bands [2–4]. Electron paramagnetic resonance (EPR) is a method of choice for the study of transition ions [5]. However, direct measurements of EPR in nanostructures are difficult because of the small total number of spins, therefore optically detected magnetic resonance (ODMR) is much better suited for the measurements in such systems [6].

In this letter the EPR spectra of the individual  $\text{Mn}^{2+}$  ions in  $\text{CdMnSe}/\text{ZnSe}$  QD's are investigated by ODMR method. It will be shown that the axial fine structure with strong positive zero-field splitting is observed for  $\text{Mn}^{2+}$  ions which is caused by the QD's low dimensionality.

The structures under investigation were grown by molecular-beam epitaxy as pseudomorphic relative to the (001) GaAs buffer layer and consisted of an upper and a lower 30 nm thick ZnSe barrier layers. They surrounded a  $\text{CdMnSe}$  insertion whose nominal thickness was 2.1 monolayers. The Mn content was  $x = 0.07$ . The  $\text{Cd}_{1-x}\text{Mn}_x\text{Se}/\text{ZnSe}$  self assembled quantum dots had a pancake shape with a lateral size ( $\leq 10$  nm) much ex-

<sup>1)</sup>e-mail: pavel.baranov@mail.ioffe.ru

ceeding their height. Details of the sample growth may be found in [7, 8].

ODMR was investigated with the 35 GHz (*Q*-band) ODMR spectrometer operating at 1.6–2 K and providing the magnetic field up to 4.5 T. The maximum microwave power in the cavity was 500 mW. The sample could be rotated around the vertical axis of the microwave cavity. Photoluminescence (PL) was excited far above the band gap with the He-Cd laser and detected using a grating monochromator and a photomultiplier tube. ODMR was detected by monitoring the intensity or circular polarization of luminescence.

The PL originates from the recombination of excitons localized in CdMnSe/ZnSe QD's and is therefore subjected to quantum confinement effects. The intensity of the emission strongly depends on magnetic field and temperature. At liquid He temperatures a large increase of the integrated PL intensity with magnetic field was observed following a shift of PL maximum [7, 8]. The energy of excitons in QD's varies because of *sp-d* interaction and finally depends on the thermal average value of the  $Mn^{2+}$  spin  $\langle S_z \rangle$  in the direction of the magnetic field *z*, i.e., on the Mn spin temperature. The PL is extremely sensitive to the polarization of the  $Mn^{2+}$  ions. The increase of PL intensity with magnetic field was explained to be evoked by a suppression of the non-radiative spin-dependent Auger process in individual  $Mn^{2+}$  ion [7, 9, 10]. The strong increase of the QD PL intensity is observed only in the Faraday geometry, much weaker one, in opposite, is observed in the Voigt geometry [7], the total angular dependence of this effect in magnetic field was not measured until now. To explain the observed anisotropy the selection rules for the energy transfer from excitons with total moment  $J=1$  (radiative level) and  $J=2$  (non-radiative level) to Mn ions were analyzed and these rules were found to be completely different [7]. The  $Mn^{2+}$  ions were suggested to be in  $T_d$  crystal field that is not the case in two-monolayers QD's.

Fig.1a shows PL spectra in zero-magnetic field and in the magnetic field of 2 T obtained at 2 K in the Faraday geometry ( $\theta=0^\circ$ ). As can be seen, the PL line shifts towards lower energies and strongly increases in intensity when magnetic field is applied. The ratio of the PL intensity *I* in magnetic field  $B=1.5$  T to that for  $B=0$   $I(B=1.5\text{ T})/I(B=0)$  vs angle  $\theta$  between a magnetic field and the [001] growth direction is presented in inset, filled circles correspond to the data of Ref. [7] obtained for Faraday and Voigt geometry ( $\theta=90^\circ$ ). The PL intensity enhance depends on the orientation of the sample in magnetic field and for the angle  $\theta=60^\circ$  the increase is approximately twice smaller compared to that

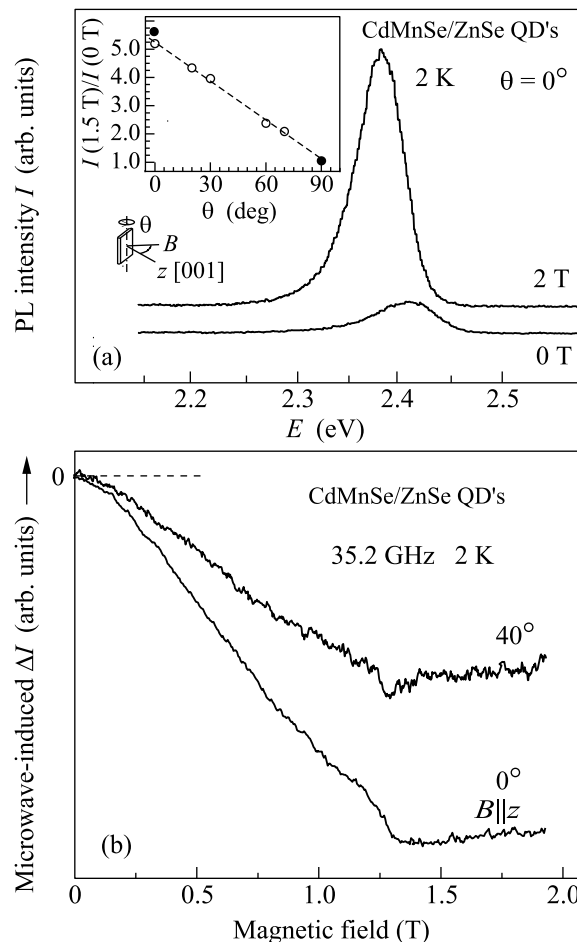


Fig.1. (a) PL spectra at 2 K for zero-magnetic field and 2 T. Inset: PL intensity  $I(B=1.5\text{ T})/I(B=0)$  vs the angle between the magnetic field and the [001] growth direction, filled circles correspond to the data of Ref. [7] for Faraday and Voigt geometry. (b) Microwave-induced variations of the PL intensity as a function of magnetic field for CdMnSe/ZnSe QD's under 35.2 GHz microwave irradiation measured at two orientations of the magnetic field

at  $\theta=0^\circ$ . An almost linear dependence is observed which obviously declines from the  $\cos \theta$  dependence of the *z* component of the magnetic field. One should take into the consideration that the ratio  $I(B)/I(0)$  increases with lowering of the excitation power [7]. In our experiments the sample is rotated in the magnetic field and the excitation power depends on the light angle of incidence  $\theta$  in opposite way and partly compensates the  $\cos \theta$  dependence. In the Faraday geometry the PL signal is strongly circularly polarized in the magnetic field.

Fig.1b presents the change of the PL intensity for CdMnSe/ZnSe QD's under 35.2 GHz microwave irradiation measured at two orientations and plotted as a function of the magnetic field. The PL intensity was recorded

while the sample was irradiated with microwaves at a fixed frequency and the magnetic field was slowly swept through the resonance. Measurements were carried out at 2 K with a microwave power of 300 mW, on-off modulated at 10 kHz. An ODMR signal corresponding to a decrease in the PL intensity was found.

Fig.2 shows the ODMR spectra of the CdMnSe/ZnSe QD's measured as a microwave-induced change of PL

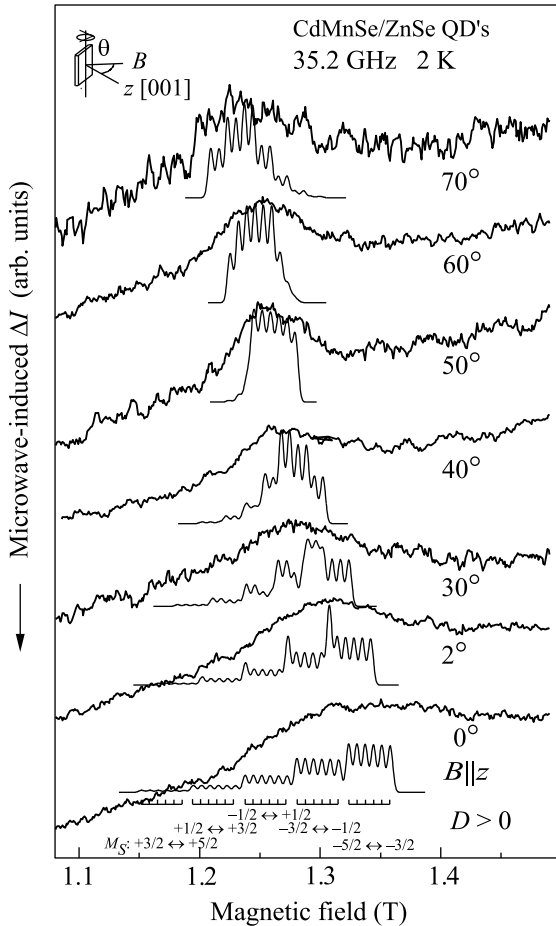


Fig.2. ODMR spectra of the CdMnSe/ZnSe QD's measured as the change of PL intensity at different orientations of the magnetic field. Measurements were carried out at 2 K with a 35.2 GHz microwave power (300 mW) on-off modulated at 10 kHz. The spectra simulated with the spin Hamiltonian parameters  $D = 200 \cdot 10^{-4} \text{ cm}^{-1}$  and line-width of 4 mT are shown under the experimental spectra

intensity at different orientations of the magnetic field. The obvious angle dependence of a broad and featureless signal is observed. The signal is definitely connected with individual  $\text{Mn}^{2+}$  ions, however,  $g$  factor of  $\text{Mn}^{2+}$  ions is known to be practically isotropic and can not give rise to an anisotropy of the ODMR signal. The EPR of  $\text{Mn}^{2+}$  ions was measured by Title [11] in hexag-

onal CdSe single crystals and was analyzed in terms of a spin Hamiltonian (without cubic terms,  $z$  axis chosen along  $c$  axis of the crystal)

$$H = \beta_e g \mathbf{B} \cdot \mathbf{S} + A \mathbf{S} \cdot \mathbf{I} + D[S_z^2 - 1/3 S(S+1)],$$

where  $\beta_e$  is the Bohr magneton,  $S=5/2$  and  $I=5/2$  are the electron and nuclear spins of  $\text{Mn}^{2+}$ , respectively,  $g=2.003$ ,  $A = -62.7 \cdot 10^{-4} \text{ cm}^{-1}$ ,  $D = 15.2 \cdot 10^{-4} \text{ cm}^{-1}$ , the linewidth is 0.5 mT at 77 K. The value of zero-field splitting  $D$  in wurtzite crystals is dependent on the trigonal (axial) distortion in these compounds. The low value of  $D$  in CdSe compared with the values found in other wurtzite crystals (e.g.,  $D = -236 \cdot 10^{-4} \text{ cm}^{-1}$  in ZnO at 300 K [12]) and its positive sign were explained by the amount of covalency [11] since the crystal fields are comparable in the wurtzite crystal family. All these parameters for  $\text{Mn}^{2+}$  ions will give the EPR spectra with an isotropic center of gravity corresponding to  $g \cong 2$ . The only case when the anisotropy could be observed is low temperatures and high microwave frequencies. An example of such anisotropic behavior which could be useful for the understanding of our ODMR results is presented in Fig.3 where 95 GHz EPR spectra of  $\text{Mn}^{2+}$

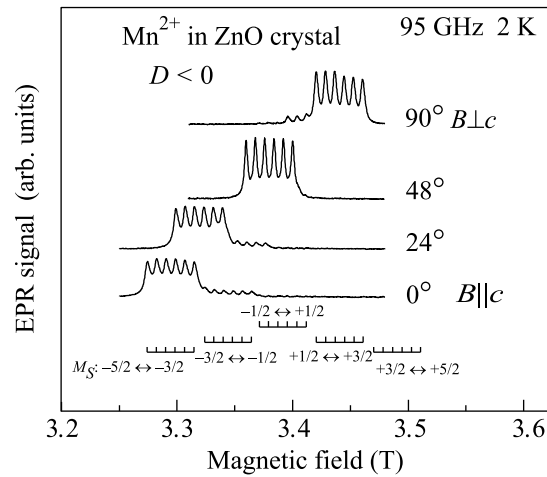


Fig.3. The high-frequency (95 GHz) EPR spectra of  $\text{Mn}^{2+}$  ions in ZnO single crystals measured at different orientations of the magnetic field at 2 K

ions observed in hexagonal ZnO crystal at 2 K are shown [13]. One can clearly see very anisotropic behavior of the center of gravity of EPR spectra in spite of isotropic  $g$  factor. The spectrum exhibits the characteristic structure of the  $S=5/2$  electron spin of the  $\text{Mn}^{2+}$  ion with an isotropic hyperfine (HF) interaction with the  $I=5/2$  nuclear spin of  $^{55}\text{Mn}$ . The bars in the bottom of Fig. 3 mark all EPR transitions which should be observed at high temperature in the orientation  $B \parallel c$ . However the

set of six strong lines corresponding to the lowest  $M_S = -5/2 \leftrightarrow M_S = -3/2$  transition dominates the spectrum because of the high Boltzmann factor at 95 GHz and 2 K. The weaker lines present a part of the sextet corresponding to the  $M_S = -3/2 \leftrightarrow M_S = -1/2$  transition.

The similar angular variation is observed for ODMR signals in CdMnSe/ZnSe QD's. In the ODMR spectra at 2 K the intensities of the fine-structure components differ strongly due to the extreme difference in the populations of the spin sublevels at this low temperature and the large Zeeman splitting. The symmetry of the fine-structure splitting due to the crystal field is consistent with a distortion from the normal cubic environment with a principal axis along [001] growth direction. This result allows us to deduce that the  $D$  parameter of the  $Mn^{2+}$  centers is about  $200 \cdot 10^{-4} \text{ cm}^{-1}$  and is positive contrary to the negative  $D$  in ZnO. The  $D$  parameter of the  $Mn^{2+}$  in CdMnSe/ZnSe QD's is much larger than that for hexagonal CdSe single crystal. The  $z$  axis is chosen to be along the growth direction [001] in CdMnSe/ZnSe QD's contrary to [111] direction for the  $c$  axis in the CdSe single crystal. Since our experiments were made at 2 K we can exclude the influence of the exchange coupled antiferromagnetic  $Mn^{2+}$ - $Mn^{2+}$  pairs and believe that we are dealing with a high-spin ground state of individual  $Mn^{2+}$  ions. The bars in the bottom of Fig.2 mark all EPR transitions which should be observed at high temperature in the orientation  $B \parallel z$ . Since we detect mainly the transitions between the lowest energy sublevels  $M_S = -5/2 \leftrightarrow M_S = -3/2$  and  $M_S = -3/2 \leftrightarrow M_S = -1/2$  whose positions strongly depend on the  $D$  value (unlike the transitions  $M_S = -1/2 \leftrightarrow M_S = +1/2$ ), the hyperfine structure is not resolved probably due to a distribution of  $D$  values. The HF structure will be totally unresolved if dispersion of  $D$  values is about 5%.

The simulated EPR signals for several orientations of magnetic field are shown under the experimental spectra in Fig.2. The spectra were simulated at Q-band using  $D = 200 \cdot 10^{-4} \text{ cm}^{-1}$  and the line-width of 4 mT, the occupation probability of the six  $Mn^{2+}$  spin states subject to the Boltzmann distribution was taken into account. The HF structure is resolved in simulated spectra since it was calculated for a fixed fine-structure parameter.

The dominant property of nanostructures is their low dimensionality. Characteristic features of carriers and fine structure of excitons were observed in such systems by ODMR [6]. The exciton levels are split in zero field in the low dimensional systems, e.g., for type II GaAs/AlAs SL's the fine-structure splitting observed is explained by low local symmetry  $C_{2v}$  of interfaces at which excitons

are localized. Thus, the zero-field splitting in SL's is caused by their low dimensionality. We conclude that the observation of  $Mn^{2+}$  fine structure in CdMnSe/ZnSe QD's is also caused by their low dimensionality. The influence of the system geometry on emission spectra was observed for exchange coupled exciton-manganese pairs in single CdMnTe/ZnTe QD's [14]. To our knowledge, until now no low symmetry effects caused by low dimensionality were observed in EPR of transition metals. The symmetry of the fine-structure splitting due to the crystal field is consistent with [001] growth direction. The unresolved character of the  $Mn^{2+}$  EPR lines seems to be caused by a size distribution of QD's and as a result the distribution of the zero-field splitting  $D$  values. In addition, the quantization axis of a QD's (as was shown in Ref. [15]) can partly decline from the structure growth axis and to contribute to the ODMR signal line-width.

The magnitude and sign of the  $D$  parameter in CdMnSe/ZnSe QD's are correlated with those for  $Mn^{2+}$  ions in alkali halides which are paired off with vacancies in the next-nearest cation site [16]. Terms quadratic in  $S$  arise from terms in the Hamiltonian for  $d$  electrons of  $Mn^{2+}$  which are quadratic in the position coordinate  $r$ . When the distance between Mn ion and the charged vacancy in Ref. [16] is compared with the QD height in our experiments, it is apparent that the quadratic terms, zero in cubic symmetry of bulk CdSe, arise since the QD shape is essentially noncubic; i.e., the size in the growth direction is much shorter than the sizes in the perpendicular plane. It should be noted that the simple crystalline field theory alone was unsuccessful in explaining the  $Mn^{2+}$  fine structure values produced by the vacancy and the importance of covalency effects was indicated [16].

In addition, the interface energy gap jump from ZnSe to CdSe occurs at a short distance. The energy-gap jump at interface in AgCl nanocrystals embedded into KCl matrix was shown in Ref. [17] to suppress the Jahn-Teller effect and to change the fine structure parameters of self-trapped excitons bound at  $Ag^{2+}$  ( $4d^9$ ) self-trapped hole.

It is of interest to perform the ODMR measurements on a single CdMnSe/ZnSe QD. In such experiments a fixed  $Mn^{2+}$  fine structure and the resolved HF structure should be observed which could be used as a new characteristic of the QD's. The fine structure effect induced with low dimensionality should be applicable to a wide range of compounds and transition ions. This effects should be taken into account in finding of  $Mn^{2+}$   $g$  factors at low temperatures and high magnetic fields.

The effect of nonresonant microwave illumination on the PL intensity (background signal in Fig.1b) corresponds only to the heating of the system by means of the microwave radiation which can be absorbed by free carriers under conditions of cyclotron resonance (optically detected cyclotron resonance [18]).

In summary, EPR of  $Mn^{2+}$  ions has been observed in CdMnSe/ZnSe QD's using optical detection. The anisotropic behavior of the center of gravity of the EPR spectra has been observed. The EPR lines corresponding to the lowest  $M_S = -5/2 \leftrightarrow M_S = -3/2$  and  $M_S = -3/2 \leftrightarrow M_S = -1/2$  transition were found to dominate the spectrum because of the high Boltzmann factor at 35 GHz and 2 K. The axial fine structure with strong positive zero-field splitting  $D \approx 200 \cdot 10^{-4} \text{ cm}^{-1}$  in CdMnSe/ZnSe QD's is concluded to be caused by their low dimensionality. The lack of the resolved HF structure of the  $Mn^{2+}$  EPR lines is caused by a size distribution of QD's and as a result the distribution of zero-field splitting  $D$  values.

This work was supported by the Programs of RAS: Spin-Dependent Effects in Solids and Spintronics; P-03 Quantum Macrophysics; Support of Innovations and Elaborations. Further support was obtained from Federal Agency for Science and Innovations under Contract # 02.513.12.3031.

1. J. K. Furdyna, J. Appl. Phys. **64**, R29 (1988).
2. A. V. Komarov, S. M. Ryabchenko, O. V. Terletskii et al., Sov. Phys. JETP **46**, 318 (1977).
3. T. Wojtovich, M. Kutrowski, G. Karczewski et al., Phys. Rev. B **59**, R10437 (1999).
4. S. J. C. H. M. van Gisbergen, M. Godlewski, R. R. Galazka et al., Phys. Rev. B **48**, 11767 (1993).
5. A. Abragam and B. Bleaney, *Electron Paramagnetic Resonance of Transition Ions*, Oxford University Press, Oxford, 1970.
6. P. G. Baranov and N. G. Romanov, Appl. Magn. Reson. **21**, 165 (2001) and references therein.
7. A. V. Chernenko, P. S. Dorozhkin, V. D. Kulakovskii et al., Phys. Rev. B **72**, 045302 (2005).
8. S. V. Ivanov, T. V. Shubina, I. V. Sedova et al., Poverkhnost'. Rentgenovskie, sinkhrotronnye i neutronnye issledovaniya **10**, 6 (2003) [Journal of Surface Investigation. X-ray, Synchrotron and Neutron Techniques **10**, 6 (2003)].
9. V. G. Abramishvili, A. M. Komarov, S. M. Ryabchenko, and Yu. G. Semenov, Solid State Commun. **78**, 1069 (1991).
10. M. Nawroski, Yu. G. Rubo, J. P. Lascaray, and D. Coquillat, Phys. Rev. B **52**, R2241 (1995).
11. R. S. Title, Phys. Rev. **130**, 17 (1963); **131**, 2503 (1963).
12. A. Hausmann, Solid State Comm. **6**, 457 (1968); **131**, 2503 (1963).
13. S. B. Orlinskii, P. G. Baranov, and J. Schmidt, unpublished results.
14. Y. Léger, L. Besombes, L. Maingault et al., Phys. Rev. Lett. **95**, 047403 (2005).
15. Yu. G. Kusrayev, B. R. Namozov, I. V. Sedova, and S. V. Ivanov, Phys. Rev. B **76**, 153307 (2007).
16. G. D. Watkins, Phys. Rev. **113**, 79 (1959).
17. P. G. Baranov, V. S. Vikhnin, N. G. Romanov, and V. A. Khramtsov, JETP Letters **72**, 329 (2000).
18. P. G. Baranov, Yu. P. Veshchunov, R. A. Zhitnikov et al., JETP Letters **26**, 249 (1977).